Relativistic Description of Exclusive Semileptonic Decays of Heavy Mesons

R.N.Faustov, V.O.Galkin and A.Yu.Mishurov

Russian Academy of Sciences, Scientific Council for Cybernetics, Vavilov Street 40, Moscow, 117333, Russia.

Abstract

Using quasipotential approach, we have studied exclusive semileptonic decays of heavy mesons with the account of relativistic effects. Due to more complete relativistic description of the s quark more precise expressions for semileptonic form factors are obtained. Various differential distributions in exclusive semileptonic decays of heavy mesons are calculated. It is argued that consistent account of relativistic effects and HQET motivated choice of the parameters of quark-antiquark potential allow to get reliable value for the ratio $A_2(0)/A_1(0)$ in the $D \to K^* l\nu_l$ decay as well as the ratio $\Gamma(D \to K^* l\nu_l)/\Gamma(D \to K l\nu_l)$. All calculated branching ratios are in accord with available experimental data.
PACS number(s): 12.39Ki, 13.20He, 13.40Hq

1 Introduction

Semileptonic decays of heavy mesons provide an important tool to investigate quark dynamics and to determine Cabibbo-Kobayshi-Maskawa (CKM) matrix elements. Hadron dynamics is contained in form factors, which are Lorentz invariant functions of q^2, the square of momentum transfer. These form factors cannot be calculated from the first principles of QCD by now. Thus various potential models, sum rules and lattice calculations have been proposed [1]–[6]. Recently considerable progress has been achieved in describing heavy meson decays by the use of heavy quark effective theory (HQET) [7]. It has been found that in the limit of infinitely heavy b and c quarks their mass and spin decouple from the dynamics of the decay and the description of a process such as $B \to Dl\nu_l$ is strongly simplified. For D decays HQET predictions are less useful, because in this case symmetry breaking corrections appear to be rather large. It is also important to note that since B and D mesons contain light quark, relativistic effects are quite significant and consistent relativistic description of heavy-light quark system is necessary.

Our relativistic quark model (RQM), has some features that make it attractive and reliable for the description of heavy mesons. Firstly, RQM provides a consistent scheme for calculation of all relativistic corrections and allows for the heavy quark $1/m_Q$ expansion. Secondly, it has been found [8] that the general structure of leading, next- to-leading and second order $1/m_Q$ corrections in RQM is in accord with the predictions of HQET. The heavy quark symmetry and QCD impose some rigid constraints on the parameters of the long-range confining potential of our model. It gives an additional motivation for the choice of the main parameters of RQM and leads us to the conclusion that the confining quark-antiquark potential in meson is predominantly Lorentz-vector (with the Pauli term), while the scalar potential is anticonfining and helps to reproduce the initial nonrelativistic potential. This model has been applied to the calculations of meson mass spectra [9], radiative decay widths [10], pseudoscalar decay constants [11], rare radiative [12] and nonleptonic [13] decay rates. Semileptonic decays of B and D mesons have been considered in our model in [14]. Here we refine our previous analysis with more complete account of relativistic effects and HQET constraints. We also consider exclusive decay spectra and q^2 dependence of form factors.

In Sect.2 we briefly describe RQM. Sect.3 is devoted to the calculation of form factors and semileptonic branching ratios and contains analytical expressions and numerical results for the differential distributions for the decays into pseudoscalar as well as vector final states. We give our conclusions in Sect.4.

2 Relativistic Quark Model

Our model is based on the quasipotential approach in quantum field theory [15]. A quark-antiquark bound system with the mass M and relativistic momentum $\mathbf{p}$ in the center of mass system is described by a single-time quasipotential wave function $\Psi_M(\mathbf{p})$, projected onto positive-energy states. This wave function satisfies the quasipotential equation

$$\left[M^2 - (\mathbf{p}^2 + m_1^2)^{1/2} - (\mathbf{p}^2 + m_2^2)^{1/2}\right] \Psi_M(\mathbf{p}) = \int \frac{d^3\mathbf{q}}{(2\pi)^3} V(\mathbf{p}, \mathbf{q}; M) \Psi_M(\mathbf{q}), \tag{1}$$

The quasipotential equation (1) can be transformed into a local Schrödinger-like equation [16]

$$\left[\frac{b^2(M)}{2\mu_R} - \frac{\mathbf{p}^2}{2\mu_R}\right] \Psi_M(\mathbf{p}) = \int \frac{d^3\mathbf{q}}{(2\pi)^3} V(\mathbf{p}, \mathbf{q}; M) \Psi_M(\mathbf{q}), \tag{2}$$

where the relativistic reduced mass is

$$\mu_R = \frac{E_1 E_2}{E_1 + E_2} = \frac{M^4 - (m_1^2 - m_2^2)^2}{4M^3}; \tag{3}$$

$$E_1 = \frac{M^2 - m_2^2 + m_1^2}{2M}; \qquad E_2 = \frac{M^2 - m_1^2 + m_2^2}{2M}; \qquad E_1 + E_2 = M.$$

and the square of the relative momentum on the mass shell is

$$b^2(M) = \frac{\left[M^2 - (m_1 + m_2)^2\right]\left[M^2 - (m_1 - m_2)^2\right]}{4M^2}, \tag{4}$$

$m_{1,2}$ are the quark masses.

Now it is necessary to construct the quasipotential $V(\mathbf{p}, \mathbf{q}; M)$ of the quark-antiquark interaction. As well known from QCD, in view of the property of asymptotic freedom the one-gluon exchange potential gives the main contribution at short distances. With the increase of the distance the long-range confining interaction becomes dominant. At present the form of this interaction cannot be established in the framework of QCD. The most general kernel of $q\bar{q}$ interaction, corresponding to the requirements of Lorentz invariance and of P and T invariance, contains [17], [18] scalar, pseudoscalar, vector, axial-vector and tensor parts. The analysis carried out in [9], [17] has shown that the leading contributions to the confining part of the potential should have a vector and scalar structure. On the basis of these arguments we have assumed that the effective interaction is the sum of the one-gluon exchange term and the mixture of long-range vector with scalar potentials. We have also assumed that at large distances quarks acquire universal nonperturbative anomalous chromomagnetic moments and thus the vector long-range potential contains the Pauli interaction. The quasipotential is defined by [9]

$$V(\mathbf{p}, \mathbf{q}; M) = \bar{u}_1(p)\bar{u}_2(-p)\left(\frac{4}{3}\alpha_s D_{\mu\nu}(\mathbf{k})\gamma_1^\mu\gamma_2^\nu + V_{conf}^V(\mathbf{k})\Gamma_1^\mu\Gamma_{2;\mu} + V_{conf}^S(\mathbf{k})\right) u_1(q)u_2(-q), \tag{5}$$

where α_s is the QCD coupling constant, $D_{\mu\nu}$ is the gluon propagator; γ_μ and $u(p)$ are the Dirac matrices and spinors; $\mathbf{k} = \mathbf{p} - \mathbf{q}$; Γ_μ is the effective vector vertex at large distances,

$$\Gamma_\mu(\mathbf{k}) = \gamma_\mu + \frac{i\kappa}{2m}\sigma_{\mu\nu}k^\nu, \tag{6}$$

κ is the anomalous chromomagnetic quark moment.

The complete expression for the quasipotential obtained from (5), (6) with the account of the relativistic corrections of order v^2/c^2 can be found in [9]. In the nonrelativistic limit vector and scalar confining potentials reduce to

$$V^V_{conf}(r) = (1-\varepsilon)(Ar+B), \qquad V^S_{conf}(r) = \varepsilon(Ar+B), \tag{7}$$

reproducing $V^{conf}_{nonrel}(r) = V^S_{conf} + V^V_{conf} = Ar + B$, where ε is the mixing coefficient.

All the parameters of our model: quark masses, parameters of linear confining potential A and B, mixing coefficient ε and anomalous chromomagnetic quark moment κ were originally fixed from the analysis of meson masses [9] and radiative decays [10]. Quark masses: m_b= 4.88 GeV; m_c= 1.55 GeV; m_s= 0.50 GeV; $m_{u,d}$= 0.33 GeV and parameters of the linear potential: A= 0.18 GeV^2; B= -0.30 GeV have standard values for quark models. The value of mixing coefficient of vector and scalar confining potentials $\varepsilon = -0.9$ has been primarily chosen from the consideration of meson radiative decays, which are rather sensitive to the Lorentz- structure of the confining potential [10]. Universal anomalous chromomagnetic moment of quarks $\kappa = -1$ has been fixed from the analysis of the fine splitting of heavy quarkonia ^3P_J states [9].

Recently, in the framework of RQM, the $1/m_Q$ expansion of the matrix elements of weak currents between pseudoscalar and vector heavy meson states has been performed [8]. It has been found that the particular structure of $1/m_Q$ corrections up to the second order predicted by HQET can be reproduced in RQM only with some specific values of κ and ε. The analysis of the first order corrections [8] allowed to fix $\kappa = -1$, while from the consideration of the second order corrections it has been obtained that mixing parameter ε should be $\varepsilon = -1$. Thus HQET, and hence QCD, imposes strong constraints on the parameters of the long-range confining potential. The obtained value of ε is very close to the previous one, determined phenomenologically from radiative decays [10] and the value of κ coincides with the result, obtained from the mass spectra [9]. Therefore, there is an important QCD and heavy quark symmetry motivation for the choice of the main parameters of our model: $\varepsilon = -1$, $\kappa = -1$.

3 Exclusive Semileptonic Decay

3.1 Form Factors and Decay Widths

For semileptonic decay $B \to A(A^*)l\nu_l$ of pseudoscalar meson B into pseudoscalar (vector) meson $A(A^*)$ the differential width can be written as

$$d\Gamma(B \to A(A^*)l\nu_l) = \frac{1}{2M_B} \mid \mathcal{A}(B \to A(A^*)l\nu_l) \mid^2 d\Phi, \tag{8}$$

where

$$d\Phi = (2\pi)^4 \delta^{(4)}\left(p_B - p_l - p_{\nu_l} - p_A\right) \prod_i \frac{d^3p_i}{(2\pi)^3 2E_i}, \qquad i = A,\, l,\, \nu_l, \tag{9}$$

p_B is four-momentum of initial meson, p_A is four-momentum of final meson, p_l and p_{ν_l} are four-momenta of lepton and neutrino respectively.

The relevant transition amplitude looks like

$$\mathcal{A}(B \to A(A^*)l\nu_l) = \langle A(A^*)l\nu_l | H_{eff} | B\rangle = \frac{G_F}{\sqrt{2}} V_{ab} L_\mu H^\mu, \tag{10}$$

where

$$H_{eff} = \frac{G_F}{\sqrt{2}} J^\mu_{hadron} J_{lepton;\mu}, \tag{11}$$

V_{ab} is the CKM matrix element connected with $b \to a$ transition.

The leptonic L_μ and hadronic H_μ currents are defined by

$$L_\mu = \bar{l}\gamma_\mu(1-\gamma_5)\nu_l, \tag{12}$$

$$H_\mu = \langle A(A^*)|\bar{a}\gamma_\mu(1-\gamma_5)b|B\rangle, \tag{13}$$

the initial meson B has the quark structure $(b\bar{q})$ and the final meson $A(A^*)$ has the quark structure $(a\bar{q})$.

The matrix element of hadron current can be expressed in terms of Lorentz-invariant form factors

a) For $0^- \to 0^-$ transition $B \to Al\nu_l$

$$\langle A(p_A)|J_\mu^V|B(p_B)\rangle = f_+(q^2)(p_A+p_B)_\mu + f_-(q^2)(p_B-p_A)_\mu; \tag{14}$$

b) For $0^- \to 1^-$ transition $B \to A^* l\nu_l$

$$\langle A^*(p_A,e)|J_\mu^V|B(p_B)\rangle = i\frac{V(q^2)}{M_A+M_B}\epsilon_{\mu\nu\rho\sigma}e^{*\nu}(p_A+p_B)^\rho(p_B-p_A)^\sigma; \tag{15}$$

$$\begin{aligned}\langle A^*(p_A,e)|J_\mu^A|B(p_B)\rangle &= (M_A+M_B)A_1(q^2)e_\mu^* - \frac{A_2(q^2)}{M_A+M_B}(e^*p_B)(p_A+p_B)_\mu \\ &+\frac{A_3(q^2)}{M_A+M_B}(e^*p_B)(p_B-p_A)_\mu;\end{aligned} \tag{16}$$

where $q = p_B - p_A$; $J_\mu^V = (\bar{a}\gamma_\mu b)$ and $J_\mu^A = (\bar{a}\gamma_\mu\gamma_5 b)$ are vector and axial parts of the weak current; e_μ is the polarization vector of A^* meson.

Since $q = p_l + p_{\nu_l}$, the terms proportional to q_ν, i.e. f_- and A_3 give contributions proportional to the lepton masses and do not influence significantly the transition amplitude, except for the case of heavy τ lepton, and thus will not be considered.

The matrix element of the local current J between bound states in the quasipotential method has the form [19]

$$\langle A|J_\mu(0)|B\rangle = \int\frac{d^3\mathbf{p}d^3\mathbf{q}}{(2\pi)^6}\bar{\Psi}_A(\mathbf{p})\Gamma_\mu(\mathbf{p},\mathbf{q})\Psi_B(\mathbf{q}), \tag{17}$$

where $\Gamma_\mu(\mathbf{p},\mathbf{q})$ is the two-particle vertex function and $\Psi_{A,B}$ are meson wave functions projected onto the positive energy quark states.

In the case of semileptonic decays $J_\mu = J_{hadron;\mu} = J_\mu^V - J_\mu^A$ is the weak quark current and in order to calculate its matrix element between meson states it is necessary to consider the contributions to Γ from Figs. 1 and 2. The vertex functions obtained from these diagrams look like

$$\Gamma_\mu^{(1)}(\mathbf{p},\mathbf{q}) = \bar{u}_a(p_1)\gamma_\mu(1-\gamma_5)u_b(q_1)(2\pi)^3\delta(\mathbf{p}_2-\mathbf{q}_2), \tag{18}$$

and

$$\begin{aligned}\Gamma_\mu^{(2)}(\mathbf{p},\mathbf{q}) &= \bar{u}_a(p_1)\bar{u}_q(p_2)\Big[\gamma_{1\mu}(1-\gamma_1^5)\frac{\Lambda_b^{(-)}(\mathbf{k})}{\varepsilon_b(k)+\varepsilon_b(p_1)}\gamma_1^0 V(\mathbf{p}_2-\mathbf{q}_2) \\ &+V(\mathbf{p}_2-\mathbf{q}_2)\frac{\Lambda_a^{(-)}(\mathbf{k}')}{\varepsilon_a(k')+\varepsilon_a(q_1)}\gamma_1^0\gamma_{1\mu}(1-\gamma_1^5)\Big]u_b(q_1)u_q(q_2),\end{aligned} \tag{19}$$

where $\mathbf{k} = \mathbf{p}_1 - \mathbf{\Delta}$; $\quad \mathbf{k}' = \mathbf{q}_1 + \mathbf{\Delta}$; $\quad \mathbf{\Delta} = \mathbf{p}_B - \mathbf{p}_A$; $\quad \varepsilon(p) = (m^2+\mathbf{p}^2)^{1/2}$;

$$\Lambda^{(-)}(p) = \frac{\varepsilon(p) - (m\gamma^0 + \gamma^0\vec{\gamma}\mathbf{p})}{2\varepsilon(p)}.$$

As one can see, the form of relativistic corrections resulting from $\Gamma_\mu^{(2)}(\mathbf{p},\mathbf{q})$ is explicitly dependent on the Lorentz-structure of quark-antiquark potential.

Our previous analysis of the semileptonic $B \to D(D^*)$ and $D \to K(K^*)$ transitions [14] was based on the assumption that we could expand (19) up to the order $\mathbf{p}^2/m^2$ with respect to both b and a quarks. This assumption proved to be quite adequate in the case of $B \to Dl\nu_l$ where both b and c quarks are heavy. However, the final s quark is not heavy enough. It would be more accurate not to expand $\Gamma_\mu^{(2)}(\mathbf{p},\mathbf{q})$ at all, but one should do it in order to perform one of the integrations in (17). Our statement is that more reliable results for semileptonic $D \to K$ decays can be obtained by using $\mathbf{p}^2/\varepsilon_a^2(p)$ expansion instead of $\mathbf{p}^2/m^2$ in (19).

It is also necessary to take into account that the wave function of final A meson $\Psi_{A,\mathbf{p}_A}(\mathbf{p})$ is connected with one in A rest frame $\Psi_{A,\mathbf{0}}(\mathbf{p})$ as follows [19]

$$\Psi_{A,\mathbf{p}_A}(\mathbf{p}) = D_a^{1/2}(R^W_{L_{\mathbf{p}_A}}) D_q^{1/2}(R^W_{L_{\mathbf{p}_A}}) \Psi_{A,\mathbf{0}}(\mathbf{p}), \tag{20}$$

where $D^{1/2}(R)$ is well-known rotation matrix and R^W is the Wigner rotation.

The meson functions in the rest frame have been calculated [20] by numerical solution of the quasipotential equation (2). However, it is more convinient to use analytical expressions for meson wave functions. The examination of numerical results for the ground state wave functions of mesons containing at least one light quark has shown that they can be well approximated by the Gaussian functions

$$\Psi_M(\mathbf{p}) \equiv \Psi_{M,\mathbf{0}}(\mathbf{p}) = \left(\frac{4\pi}{\beta_M^2}\right)^{3/4} \exp\left(-\frac{\mathbf{p}^2}{2\beta_M^2}\right), \tag{21}$$

with the deviation less than 5%.

The parameters are

$$\begin{aligned} &\beta_B = 0.41\,\mathrm{GeV}; \qquad \beta_K = \beta_{K^*} = 0.33\,\mathrm{GeV}; \qquad \beta_\phi = 0.36\,\mathrm{GeV}; \\ &\beta_D = 0.38\,\mathrm{GeV}; \qquad \beta_{D_s} = 0.44\,\mathrm{GeV} \end{aligned} \tag{22}$$

In the B meson rest frame equations (14)–(16) can be written in the three-dimensional form

a) For $0^- \to 0^-$ transition $B \to Al\nu_l$

$$\langle A(p_A)|J_0^V|B(p_B)\rangle = f_+(q^2)(M_B + E_A) + f_-(q^2)(M_B - E_A), \tag{23}$$

$$\langle A(p_A)|\mathbf{J}^V|B(p_B)\rangle = (f_-(q^2) - f_+(q^2))\mathbf{\Delta}, \tag{24}$$

b) For $0^- \to 1^-$ transition $B \to A^* l\nu_l$

$$\langle A^*(p_A,e)|J_0^V|B(p_B)\rangle = i\frac{V(q^2)}{M_A+M_B}\epsilon_{0\nu\rho\sigma}\tilde{e}^{*\nu}(p_A+p_B)^\rho(p_B-p_A)^\sigma = 0, \tag{25}$$

$$\langle A^*(p_A,e)|\mathbf{J}^V|B(p_B)\rangle = i\frac{2M_B}{M_A+M_B}V(q^2)\left[\tilde{\mathbf{e}}^*\mathbf{\Delta}\right], \tag{26}$$

$$\begin{aligned} \langle A^*(p_A,e)|J_0^A|B(p_B)\rangle = \tilde{e}_0^*\Big(&A_1(q^2)(M_A+M_B) - A_2(q^2)\frac{M_B}{M_A+M_B}(M_B+E_A) \\ &+A_3(q^2)\frac{M_B}{M_A+M_B}(M_B-E_A)\Big), \end{aligned} \tag{27}$$

$$\langle A^*(p_A,e)|\mathbf{J}^A|B(p_B)\rangle = A_1(q^2)(M_A+M_B)\tilde{\mathbf{e}} - \mathbf{\Delta}\tilde{e}_0^*\frac{M_B}{M_A+M_B}(A_2(q^2)+A_3(q^2)), \tag{28}$$

where $e_\mu = (0,\mathbf{e})$ is the polarization vector of A^* meson in its rest frame, $\tilde{e}_\mu$ is the vector obtained from e_μ by the Lorentz transformation $L_{\mathbf{\Delta}}$

$$\tilde{e}_\mu = L_{\mathbf{\Delta}} e_\mu. \tag{29}$$

The components of $\tilde{e}_\mu$ look like

$$\tilde{e}_0 = \frac{\mathbf{e}\mathbf{\Delta}}{M_A}, \qquad \tilde{\mathbf{e}} = \mathbf{e} + \frac{\mathbf{\Delta}(\mathbf{\Delta}\mathbf{e})}{M_A(E_A+M_A)} = \mathbf{e} + \tilde{e}_0\frac{\mathbf{\Delta}}{E_A+M_A}. \tag{30}$$

Equations (23), (24) and (25)–(28) determine form factors f_+, f_- and V, A_1, A_2, A_3 respectively.

Substituting the vertex functions (18) and (19), with the account of wave function transformation (20) and quasipotential equation (1) in the matrix element (17) and using eqs. (23), (24) and (25)–(28) we get the following expressions at $q^2 = q^2_{max} = (M_B - M_A)^2$ point

$$
\begin{aligned}
f_+(q^2_{max}) &= f_+^{(1)}(q^2_{max}) + \varepsilon f_{+S}^{(2)}(q^2_{max}) + (1-\varepsilon) f_{+V}^{(2)}(q^2_{max}), && (31)\\
A_1(q^2_{max}) &= A_1^{(1)}(q^2_{max}) + \varepsilon A_{1S}^{(2)}(q^2_{max}) + (1-\varepsilon) A_{1V}^{(2)}(q^2_{max}), && (32)\\
A_2(q^2_{max}) &= A_2^{(1)}(q^2_{max}) + \varepsilon A_{2S}^{(2)}(q^2_{max}) + (1-\varepsilon) A_{2V}^{(2)}(q^2_{max}), && (33)\\
V(q^2_{max}) &= V^{(1)}(q^2_{max}) + \varepsilon V_S^{(2)}(q^2_{max}) + (1-\varepsilon) V_V^{(2)}(q^2_{max}), && (34)
\end{aligned}
$$

where $f_+^{(1)}$, $f_{+S,V}^{(2)}$, $A_{1,2}^{(1)}$, $A_{1S,V}^{2}$, $A_{2S,V}^{(2)}$, $V^{(1)}$ and $V_{S,V}^{(2)}$ are given in Appendix A. In (31)–(34) indeces (1) and (2) correspond to the diagrams in Figs. 1 and 2, S and V correspond to the scalar and vector potentials of quark-interaction.

Now our concern is to find q^2 dependence of the form factors. Components of axial and vector currents can be expressed in terms of two functions $F_1(\mathbf{\Delta})$ and $F_2(\mathbf{\Delta})$, $\mathbf{\Delta} = \mathbf{p}_B - \mathbf{p}_A$,

$$
\begin{aligned}
J_0^V(\mathbf{\Delta}) &= F_2(\mathbf{\Delta}), && (35)\\
\mathbf{J}^V(\mathbf{\Delta}) &= \frac{\mathbf{\Delta} + i[\mathbf{e}^*\mathbf{\Delta}]}{2m_a} F_1(\mathbf{\Delta}), && (36)\\
J_0^A(\mathbf{\Delta}) &= \frac{(\mathbf{e}^*\mathbf{\Delta})}{2m_a} F_1(\mathbf{\Delta}), && (37)\\
\mathbf{J}^A(\mathbf{\Delta}) &= \mathbf{e}^* F_2(\Delta). && (38)
\end{aligned}
$$

Functions F_1 and F_2 arise from the lower and the upper components of Dirac spinors

$$
u_a^\lambda(p) = \left(\frac{\varepsilon_a(p) + m_a}{2\varepsilon_a(p)}\right)^{1/2} \begin{pmatrix} 1 \\ \frac{\vec{\sigma}\mathbf{p}}{\varepsilon_a(p)+m_a} \end{pmatrix} \chi^\lambda, \qquad (39)
$$

and are equal to

$$
\begin{aligned}
F_1(\mathbf{\Delta}) &= \frac{2m_a}{\varepsilon_a(\mathbf{q}+\mathbf{\Delta}) + m_a} \left(\frac{\varepsilon_a(\mathbf{q}+\mathbf{\Delta}) + m_a}{2\varepsilon_a(\mathbf{q}+\mathbf{\Delta})}\right)^{1/2} \sqrt{\frac{E_A}{M_A}}, && (40)\\
F_2(\mathbf{\Delta}) &= \left(\frac{\varepsilon_a(\mathbf{q}+\mathbf{\Delta}) + m_a}{2\varepsilon_a(\mathbf{q}+\mathbf{\Delta})}\right)^{1/2} \sqrt{\frac{E_A}{M_A}}. && (41)
\end{aligned}
$$

Near $q^2 = q^2_{max}$ it can be written as

$$
\begin{aligned}
F_1(\mathbf{\Delta}) &= \frac{\sqrt{2}(1 + \mathbf{\Delta}^2/M_A^2)^{1/2}}{\left(1 + \mathbf{\Delta}^2/m_a^2 + \sqrt{1 + \mathbf{\Delta}^2/m_a^2}\right)^{1/2}}, && (42)\\
F_2(\mathbf{\Delta}) &= \frac{1}{\sqrt{2}} \left(1 + \frac{1}{\sqrt{1 + \mathbf{\Delta}^2/m_a^2}}\right)^{1/2} \left(1 + \frac{\mathbf{\Delta}^2}{M_A^2}\right)^{1/2}. && (43)
\end{aligned}
$$

The dependence of the formfactors on the momentum transfer is fixed by extrapolating their behavior near $q^2 = q^2_{max}$ ($\mathbf{\Delta} = 0$) point over the kinematically allowed region

$$
\begin{aligned}
f_+(\mathbf{\Delta}) &= f_+(0) I(\mathbf{\Delta}) F_1(\mathbf{\Delta}), && (44)\\
A_1(\mathbf{\Delta}) &= A_1(0) I(\mathbf{\Delta}) F_2(\mathbf{\Delta}), && (45)\\
A_2(\mathbf{\Delta}) &= A_2(0) I(\mathbf{\Delta}) F_1(\mathbf{\Delta}), && (46)\\
V(\mathbf{\Delta}) &= V(0) I(\mathbf{\Delta}) F_1(\mathbf{\Delta}), && (47)
\end{aligned}
$$

where

$$I(\mathbf{\Delta}) = \int \frac{d^3\mathbf{p}}{(2\pi)^3}\bar{\Psi}_A\left(\mathbf{p} + \frac{2\varepsilon_q}{E_A + M_A}\mathbf{\Delta}\right)\Psi_B(\mathbf{p}). \tag{48}$$

Introducing the variable

$$w \equiv v_A v_B = \frac{M_B^2 + M_A^2 - q^2}{2M_A M_B}, \tag{49}$$

where v_A and v_B are meson velocities, and taking into account that

$$\mathbf{\Delta}^2 = (\mathbf{p}_B - \mathbf{p}_A)^2 = \frac{(M_B^2 + M_A^2 - q^2)^2}{4M_B^2} - M_A^2 = M_A^2(w^2 - 1), \tag{50}$$

we can rewrite (44)–(47) in the form

$$f_+(w) = f_+(1)I(w)\left(\frac{2}{w+1}\right)^{1/2}, \tag{51}$$

$$A_1(w) = A_1(1)I(w)\left(\frac{w+1}{2}\right)^{1/2}, \tag{52}$$

$$A_2(w) = A_2(1)I(w)\left(\frac{2}{w+1}\right)^{1/2}, \tag{53}$$

$$V(w) = V(1)I(w)\left(\frac{2}{w+1}\right)^{1/2}, \tag{54}$$

Substitution of the Gaussian wave functions (21) in (48) results in

$$I(w) = \exp\left(-\frac{2\bar{\Lambda}^2}{\beta_{M_A}^2 + \beta_{M_B}^2}\frac{w-1}{w+1}\right)I(1), \tag{55}$$

where $\bar{\Lambda} =< \varepsilon_q >$ is a mean value of light quark energy inside meson. In our model $\bar{\Lambda}$ corresponds to HQET parameter $\bar{\Lambda} = M - m_Q$, which determines the energy carried by light degrees of freedom, and is found to be [9]: $\bar{\Lambda} = 0.54$ GeV.

In the limit of infinitely heavy b and a quarks the w dependence of eqs. (51)–(55) is determined by the Isgur-Wise function of our model

$$\xi(w) = \left(\frac{2}{w+1}\right)^{1/2}\exp\left(-\frac{\bar{\Lambda}^2}{\beta^2}\frac{w-1}{w+1}\right) \tag{56}$$

and the ratios of form factors satisfy all constraints imposed by HQET [7].

Using (31)–(34) and (**??**)–(**??**) we have calculated form factors for $B \to D(D^*)l\nu_l$, $D \to K(K^*)l\nu_l$ and $D_s \to \varphi l\nu_l$ exclusive decays. The results obtained in our model for $D \to K(K^*)l\nu_l$ are compared with appropriate experimental data and various model predictions in Table 1. New values of form factors for $D \to K(K^*)l\nu_l$ are somewhat larger then our previous results [14] because of more consistent relativistic treatment of s quark and slight change in the value of the mixing coefficient ε. Note that while the other potential models agree with the experimental determination of $V(0)$, but fail to predict $A_1(0)$ and $A_2(0)$, our model predicts correct values of $A_1(0)$ and $A_2(0)$, but gives too low value of $V(0)$. The reason for that is not clear. The contribution from form factor $V(0)$ in the total width is kinematicaly suppresed. So, despite the above mentioned descripancy, we have got the $D \to K^* l\nu_l$ width in accord with experimental data.

The ratios of form factors $R_2 = A_2(0)/A_1(0)$ and $R_V = V(0)/A_1(0)$ are given in Table 2.

The obtained branching ratios are

$$B(D^0 \to K^{*-}e^+\nu_e) = 1.9\%, \text{ for } \tau_{D^0} = 0.415 \times 10^{-12}\text{s};$$

$$B(D^+ \to \bar{K}^{*^0} e^+ \nu_e) = 4.9\%, \text{ for } \tau_{D^+} = 1.060 \times 10^{-12}\text{s};$$

to be compared with the experimental average data [22]

$$B^{exp}(D^0 \to K^{*^-} e^+ \nu_e) = (2.0 \pm 0.4)\%,$$
$$B^{exp}(D^+ \to \bar{K}^{*^0} e^+ \nu_e) = (4.8 \pm 0.4)\%.$$

The ratio $\Gamma(D \to K^* e\nu_e)/\Gamma(D \to Ke\nu_e)$ and the ratio of the longitudinal and transverse decay widths Γ_L/Γ_T also agree well with experiment (see Table 3).

For $D_s \to \varphi l\nu_l$ decay form factors our predictions are

$$A_1(0) = 0.63,\ A_2(0) = 0.35 \text{ and } V(0) = 1.06.$$

As experiment provides us with R_2 and R_V ratios for $D_s \to \varphi l\nu_l$, we compare it with predicted values in Table 4. It is not clear why experimental ratio R_2 for $D_s \to \varphi l\nu_l$ so differs from that of $D \to K^* l\nu_l$. In RQM we get approximately equal ratios R_2 for both decays, because general structure and the signs of the potential-dependent corrections in (31)–(34) are almost the same. It can be expected that the experimental results for $D_s \to \varphi l\nu_l$ form factor ratios will change in the future. Anyway, the experimental uncertainties are still too large to conclude that there is a serious descripancy between RQM and the experimental data in this case.

For $D_s \to \varphi l\nu_l$ branching ratio we have $B(D_s \to \varphi l\nu_l) = 2.5\%$, while experiment gives $B^{exp}(D_s \to \varphi l\nu_l) = (1.88 \pm 0.29)\%$ [22].

In $B \to D^* l\nu_l$ decay, since both b and c quarks are heavy, relativistic corrections are not so significant, but the Lorentz- structure of quark-antiquark potential has an important influence on the values of form factors. We have found our results for R_2 and R_V to be in a good agreement with the experimental data [23] and HQET-based predictions [25]. Measurments and predictions for the ratios of the form factors for $B \to D^* l\nu_l$, evaluated at $q^2 = q^2_{max}$, are shown in Table 5. We have obtained the following results for $B \to D^* l\nu_l$ and $B \to Dl\nu_l$ branching ratios

$$B(B \to D^* l\nu_l) = 33.8 \times |V_{bc}|^2,\ B(B \to Dl\nu_l) = 19.8 \times |V_{bc}|^2, \text{ for } \tau_{B^0} = 1.5 \times 10^{-12}\text{s}.$$

It should be compared to the experimental data

$$B(B^0 \to D^- e^+ \nu_e) = (2.0 \pm 0.7 \pm 0.6)\% \text{ ARGUS [26]}$$
$$B(B^0 \to D^- e^+ \nu_e) = (1.8 \pm 0.6 \pm 0.3)\% \text{ CLEO- I [27]}$$
$$B(B^0 \to D^{*-} e^+ \nu_e) = (4.7 \pm 0.5 \pm 0.5)\% \text{ ARGUS [28]}$$
$$B(B^0 \to D^{*-} e^+ \nu_e) = (4.0 \pm 0.4 \pm 0.6)\% \text{ CLEO- I [27]}.$$

As a result we can extract the value of CKM matrix element V_{cb}

$$|V_{cb}| = 0.036 \pm 0.004.$$

3.2 Differential Distributions

The differential decay rate [21] can be expressed in terms of two dimensionless variables $x = E_l/M_B$ and $w = v_A v_B$, where E_l is the lepton energy

$$\frac{d^2\Gamma}{dxdw} = \frac{|V_{ab}|^2 G_F^2 M_B^5}{32\pi^3}\Big[\Big(\frac{2M_A}{M_B}w - 1 - \rho\Big)\Big(W_1(w) - 2W_3(w)\big(1 - 2x - \frac{M_A}{M_B}w\big)\Big) + 2W_2(w)\Big(\rho + (1-2x)^2 - \frac{2M_A}{M_B}w(1-2x)\Big)\Big], \quad (57)$$

Here $W_{1,2,3}(w)$ are connected with semileptonic form factors

a) For $0^- \to 0^-$ transition

$$W_1(w) = 0, \quad (58)$$
$$W_2(w) = \frac{2M_A}{M_B}|f_+(w)|^2, \quad (59)$$
$$W_3(w) = 0, \quad (60)$$

b) For $0^- \to 1^-$ transition

$$W_1(w) = \frac{2M_A}{M_B}\left(1+\frac{M_A}{M_B}\right)^2 A_1^2(w) + \frac{2M_A}{M_B}\frac{4M_A^2}{(M_A+M_B)^2}V^2(w)(w^2-1), \quad (61)$$

$$W_2(w) = \frac{M_B}{2M_A}\left(1+\frac{M_A}{M_B}\right)^2 A_1^2(w) - \frac{2M_AM_B}{M_A+M_B}V^2(w)\left(1+\rho-\frac{2M_A}{M_B}w\right)$$
$$+2A_1(w)A_2(w)\left(\frac{M_A}{M_B}-w\right) + \frac{2M_AM_B}{(M_A+M_B)^2}A_2^2(w)(w^2-1), \quad (62)$$

$$W_3(w) = \frac{4M_A}{M_B}A_1(w)V(w). \quad (63)$$

The kinematiclly allowed region is presented in Fig. 3 where the lower bound curve $w_m(x)$ has the following shape

$$w_m(x) = \frac{M_B}{2M_A}(1-2x) + \frac{M_A}{2M_B}\frac{1}{1-2x}. \quad (64)$$

The analytical expression for $d\Gamma/dx$ distribution depends on q^2 behavior of form factors. Using (51)–(55), we obtain after the integration over w

$$\frac{d\Gamma}{dx} = \frac{G_F^2|V_{cb}|^2M_B^5}{32\pi^3}\left[e^{-\alpha\frac{w_m(x)-1}{w_m(x)+1}}K_1(x) + \sinh(\alpha\chi_-(x))e^{-\alpha\chi_+(x)}K_2(x) + K_3(x)\int_{w_m(x)}^{w_0}dw\, e^{-\alpha\frac{w-1}{w+1}}\right], \quad (65)$$

where

$$\chi_-(x) = \frac{4M_AM_B^3}{(M_A+M_B)^4}\frac{x(1-R)}{1-\frac{2M_B^2}{(M_A+M_B)^2}x(1-R)}, \quad (66)$$

$$\chi_+(x) = \left(\frac{M_B-M_A}{M_B+M_A}\right)^2\frac{1-\frac{M_A^2+M_B^2}{M_B^2-M_A^2}\frac{2M_B^2}{M_B^2-M_A^2}x(1-R)}{1-\frac{2M_B^2}{M_B^2-M_A^2}x(1-R)}, \quad (67)$$

$$R = \frac{\rho}{1-2x}, \quad \rho = \frac{M_A^2}{M_B^2}, \quad \alpha = \frac{4\bar{\Lambda}^2}{\beta_{M_A}^2+\beta_{M_B}^2}, \quad w_0 = \frac{M_B^2+M_A^2}{2M_AM_B}.$$

Functions $K_{1,2,3}(x)$ take different forms for $0^- \to 0^-$ and $0^- \to 1^-$ decays and are given in Appedix B.

The $(1/\Gamma)(d\Gamma/dx)$ distributions for $B \to D(D^*)l\nu_l$, $D \to K(K^*)l\nu_l$ and $D_s \to \varphi l\nu_l$ decays are shown in Figs. 4– 6. All curves are normalised by the corresponding decay width Γ, i.e. the area under each curve is equal to 1.

4 Conclusion

Using the quasipotential approach, we have obtained the expressions for semileptonic decay form factors with the consistent account of relativistic effects. This account includes more careful consideration of the s quark contribution than it was in our previous work [14] and results in the small shift in the values of $D \to K(K^*)l\nu_l$ decay form factors, which are in a good agreement with measurments. Our model provides more accurate values for the ratio $A_2(0)/A_1(0)$ in the $D \to K(K^*)l\nu_l$ decay and for the ratio $\Gamma(D \to K^*l\nu_l)/\Gamma(D \to Kl\nu_l)$ in comparison with the other models. We have also calculated form factors and branching ratios for $B \to D(D^*)l\nu_l$, $D \to K(K^*)l\nu_l$ and $D_s \to \varphi l\nu_l$. The extracted value of $|V_{cb}| = 0.036 \pm 0.003$ is lower than the previous one [14] because of the changes in the form factors as well as in the B meson lifetime. We should emphasize that in order to get reliable results for D meson semileptonic decays it is necessary to take into consideration all possible relativistic effects, including the transformation of meson wave function (20) from the rest frame, which is ignored in many quark models.

The proposed q^2 dependence of the form factors is used for the determination of differential semileptonic distributions in the case of pseudoscalar and vector final states.

It should be noted that obtained expressions for semileptonic form factors are valid for all B and D meson decays, except the decays into mesons containing two light quarks (π, ρ mesons), where one cannot expand in either $\mathbf{p}^2/m^2$ or $\mathbf{p}^2/\varepsilon^2$ at $q^2 = q^2_{max}$ point in the vertex function (19). The solution of this problem is proposed in [34].

The analysis has shown that Lorentz-structure of quark-antiquark potential plays an important role in heavy meson semileptonic decays. We have got experimentally motivated and HQET based arguments to conclude that the confining potential has predominantly Lorentz-vector (with Pauli-term) structure $\varepsilon = -1$. Assuming also long-range anomalous chromomagnetic moment of quark to be $\kappa = -1$ we have obtained satisfactory description of all considered B and D semileptonic decays.

We argue that small number of parameters, most of which were fixed previously, and an agreement with HQET for the structure of leading, subleading and second order terms in $1/m_Q$ expansion make RQM a reliable tool for the investigation of heavy meson physics.

In this paper we have restricted ourselves with $0^- \to 0^-$ and $0^- \to 1^-$ transitions. One more practically important case of the decay into P wave final state (i.e. $B \to D^{**} l\nu_l$) will be considered in the future.

Acknowledgments

We would like to thank B.A.Arbuzov, M.Beyer, A.G.Grozin, J.G.Körner, T.Mannel, V.A.Matveev, M.Neubert, V.I.Savrin, and A.I.Studenikin for the interest in our work and helpful discussions. We are also appreciate the help of G.G.Likhachev in preparation of this paper for publication and wish to thank the Interregional Centre for Advanced Studies (Moscow) for the kind hospitality during all stages of this work. This work was supported in part by the Russian Foundation for Fundamental Research under Grant No. 94-02-03300-a.

Appendix A. Exclusive Semileptonic Decay Form Factors at $q^2 = q^2_{max}$ point

arXiv note - added Dec99 - TeX source for this appendix was corrupt on initial submission, changed to verbatim environment so that the rest of the paper can be processed.

```
\medskip
\begin{eqnarray}
\label{35}
\nonumber
f_+^{(1)}(\qm)&=&\sqrt{\frac{M_A}{M_B}}\int\frac{d^3{\bf p}}{(2\pi)^3}
\bar\Psi_A({\bf
p})\left(\frac{\varepsilon_a+m_a}{2\varepsilon_a}\right)^{1/2}
\Bigg[1+\frac{M_B-M_A}{\varepsilon_a+m_a}
-\frac{{\bf p}^2}{8}\bigg(\frac{1}{m_b^2}
-\frac{4}{m_b(\varepsilon_a+m_a)}\\
\nonumber
&&+\frac{M_B-
M_A}{\varepsilon_a+m_a}\Big(\frac{1}{m_b^2}+\frac{4}{\varepsilon_a
(\varepsilon_a+m_a)}+\frac{2}{3\varepsilon_am_a}\Big)+\frac{4}{3}\frac
\nonumber
&&\times\Big(\frac{1}{\varepsilon_a+m_a}-
\frac{1}{2m_b}\Big)\frac{\varepsilon_a
-\varepsilon_q}{\varepsilon_a \varepsilon_q} \bigg)
+\frac{M_B-M_A}{3}\bigg(\frac{1}{\varepsilon_a+m_a}+
\frac{1}{2m_b}\\
&&-\frac{{\bf p}^2}{8m_b^2}\Big(
\frac{1}{\varepsilon_a+m_a}+\frac{3}{2m_b}
\Big)\Bigg)\frac{\varepsilon_q}{M_A}({\bf p}\overleftarrow
{\frac{\partial}{\partial{\bf p}}})\Bigg]\Psi_B({\bf p}),\\
\label{36}
\nonumber
f_{+S}^{(2)}(\qm)&=&\sqrt{\frac{M_A}{M_B}}\int\frac{d^3{\bf
p}}{(2\pi)^3}
\bar\Psi_A({\bf
p})\left(\frac{\varepsilon_a+m_a}{2\varepsilon_a}\right)^{1/2}
\Bigg[-\frac{M_B-M_A}{2\varepsilon_a}\frac{M_B-\varepsilon_b-
\varepsilon_q}
{\varepsilon_a}+
\frac{M_B-M_A}{12\varepsilon_a}{\bf p}^2\\
\nonumber
&&\times\Big(\frac{1}{\varepsilon_a^2}+\frac{1}{m_b^2}\Big)-
\frac{M_B-M_A}{12}\Big(\frac{1}{\varepsilon_a^2}+\frac{1}{m_b^2}\Big)
\big(M_B+M_A-\varepsilon_b-\varepsilon_a-2\varepsilon_q\big)\\
&&\times\frac{\varepsilon_q}{M_A}({\bf p}\overleftarrow
{\frac{\partial}{\partial{\bf p}}})\Bigg]\Psi_B({\bf p}),\\
\label{37}
\nonumber
f_{+V}^{(2)}(\qm)&=&\sqrt{\frac{M_A}{M_B}}\int\frac{d^3{\bf
p}}{(2\pi)^3}
\bar\Psi_A({\bf
p})\left(\frac{\varepsilon_a+m_a}{2\varepsilon_a}\right)^{1/2}
```

```
\Bigg[\frac{M_B-M_A}{\varepsilon_a}\frac{{\bf
p}^2}{12}\bigg((1+\kappa)
\Big(\frac{1}{\varepsilon_a^2}-\frac{1}{m_b^2}\Big)\\
\nonumber
&&-
\frac{1}{\varepsilon_q}\Big(\frac{2}{\varepsilon_a+m_a}+\frac{1}{m_b}
\Big)\bigg)+
\frac{M_B-M_A}{12}(1+\kappa)\Big(\frac{1}{\varepsilon_a^2}-
\frac{1}{m_b^2}
\Big)\big(M_B-M_A-\varepsilon_q+\varepsilon_a\big)\\
\nonumber
&&\times\frac{\varepsilon_q}{M_A}({\bf p}\overleftarrow
{\frac{\partial}{\partial{\bf p}}})
+\frac{M_B-M_A}{6\varepsilon_q}\Big(\frac{1}{\varepsilon_a+m_a}
+\frac{1}{2m_b}\Big)\big(M_B+M_A-\varepsilon_b-\varepsilon_a-
2\varepsilon_q\big)\\
&&\times\frac{\varepsilon_q}{M_A}({\bf p}\overleftarrow
{\frac{\partial}{\partial{\bf p}}})\Bigg]\Psi_B({\bf p}),\\
\nonumber
A_1^{(1)}(\qm)&=&(M_A+M_B)\sqrt{4M_AM_B}\int\frac{d^3{\bf
p}}{(2\pi)^3}
\bar\Psi_A({\bf
p})\left(\frac{\varepsilon_a+m_a}{2\varepsilon_a}\right)^{1/2}
\bigg(1-\frac{{\bf p}^2}{8}\Big(\frac{1}{m_b^2}\\
&&+\frac{4}{3(\varepsilon_a+m_a)m_b}\Big)\bigg)\Psi_B({\bf p}),\\
\label{39}
A_{1S}^{(2)}(\qm)&=&A_{1V}^{(2)}(\qm)=0,\\
\label{40}
\nonumber
A_2^{(1)}(\qm)&=&\frac{1}{(M_A+M_B)\sqrt{4M_AM_B}}\int\frac{d^3{\bf
p}}
{(2\pi)^3}\bar\Psi_A({\bf
p})\left(\frac{\varepsilon_a+m_a}{2\varepsilon_a}
\right)^{1/2}\Bigg[\bigg(1+\frac{M_A}{M_B}\bigg)\\
\nonumber
&&\times\bigg(1
-\frac{{\bf
p}^2}{2}\Big(\frac{1}{4m_b^2}+\frac{1}{3m_b(\varepsilon_a+m_a)}
\Big)\bigg)-
\frac{2M_A^2}{M_B(\varepsilon_a+m_a)}\bigg(1-\frac{{\bf p}^2}{8}
\Big(\frac{1}{m_b^2}\\
\nonumber
&&+\frac{4}{\varepsilon_a(\varepsilon_a+m_a)}+
\frac{2}{3\varepsilon_am_b}\Big)
-\frac{{\bf p}^2}{6M_A\varepsilon_a}
\Big(1+\frac{\varepsilon_a+m_a}{2m_b}\Big)\bigg)\\
\nonumber
&&-\frac{2M_A\varepsilon_q}{(\varepsilon_a+m_a)M_B}\bigg(
\frac{1}{3}\Big(1+\frac{\varepsilon_a+m_a}{2m_b}
-\frac{{\bf p}^2}{8m_b^2}
\Big(1+\frac{3(\varepsilon_a+m_a)}{2m_b}\Big)\Big)\\
```

```
&&+\frac{M_B-M_A}{3m_b}\Big(1-\frac{3{\bf p}^2}{8m_b^2}\Big)\bigg)
({\bf p}\overleftarrow
{\frac{\partial}{\partial{\bf p}}})\Bigg]\Psi_B({\bf p}),\\
\label{41}
\nonumber
 A_{2S}^{(2)}(\qm)&=&\frac{1}{(M_A+M_B)\sqrt{4M_AM_B}}\int\frac{d^3{\bf
{(2\pi)^3}\bar\Psi_A({\bf
p})\left(\frac{\varepsilon_a+m_a}{2\varepsilon_a}
\right)^{1/2}\frac{M_A^2}{\varepsilon_aM_B}\Bigg[-\frac{M_B-
\varepsilon_b
-\varepsilon_q}{\varepsilon_a}\\
\nonumber
&&+\frac{{\bf
p}^2}{6}\Big(\frac{1}{\varepsilon_a^2}+\frac{1}{m_b^2}\Big)-
\frac{\varepsilon_a}{6}\big(M_B+M_A-\varepsilon_b-\varepsilon_a-
2\varepsilon_q\big)
\Big(\frac{1}{\varepsilon_a^2}+\frac{1}{m_b^2}\Big)\frac{\varepsilon_q
{M_A}({\bf p}\overleftarrow
{\frac{\partial}{\partial{\bf p}}})\Bigg]\Psi_B({\bf p}),\\
\\
\label{42}
\nonumber
A_{2V}^{(2)}(\qm)&=&\frac{1}{(M_A+M_B)\sqrt{4M_AM_B}}\int\frac{d^3{\bf
{(2\pi)^3}\bar\Psi_A({\bf
p})\left(\frac{\varepsilon_a+m_a}{2\varepsilon_a}
\right)^{1/2}\Bigg[\frac{M_A^2}{\varepsilon_aM_B}\bigg(\frac{{\bf
p}^2}{6}
(1+\kappa)\\
\nonumber
&&\times\Big(\frac{1}{\varepsilon_a^2}-\frac{1}{m_b^2}\Big)+
\frac{\varepsilon_a}{6}\big(M_B-M_A-\varepsilon_b+\varepsilon_a\big)
(1+\kappa)\Big(\frac{1}{\varepsilon_a^2}-\frac{1}{m_b^2}\Big)
\frac{\varepsilon_q}{M_A}({\bf p}\overleftarrow
{\frac{\partial}{\partial{\bf p}}})\bigg)\\
&&-\frac{{\bf p}^2}{6\varepsilon_q}
\nonumber
\Big(\frac{2}{\varepsilon_a+m_a}
+\frac{1}{m_b}\Big)+
\frac{\varepsilon_a}{6M_A}\Big(\frac{2}{\varepsilon_a+m_a}+\frac{1}{m_
&&\times\big(M_B+M_A-\varepsilon_b-\varepsilon_a-2\varepsilon_q\big)
({\bf p}\overleftarrow
{\frac{\partial}{\partial{\bf p}}})\Bigg]\Psi_B({\bf p}),\\
\label{43}
\nonumber
V^{(1)}(q^2_{max})&=&\frac{1}{M_A+M_B}\sqrt{\frac{M_A}{M_B}}\int\frac{
{(2\pi)^3}\bar\Psi_A({\bf
p})\left(\frac{\varepsilon_a+m_a}{2\varepsilon_a}
\right)^{1/2}\frac{1}{\varepsilon_a+m_a}\Bigg[1-\frac{{\bf p}^2}{8}
\Big(\frac{1}{m_b^2}\\
\nonumber
&&+\frac{4}{\varepsilon_a(m_a+\varepsilon_a)}
```

```
-\frac{2}{3\varepsilon_am_b}\Big)-
\frac{{\bf p}^2}{12M_A}\Big(1+\frac{\varepsilon_a+m_a}{2m_b}\Big)
\frac{\varepsilon_a+\varepsilon_q}{\varepsilon_a\varepsilon_q}-
\frac{{\bf p}^2}{12M_A\varepsilon_a}\Big(1-
\frac{\varepsilon_a+m_a}{2m_b}\Big)\\
&&+\frac{1}{3}\Big(1-\frac{\varepsilon_a+m_a}{2m_b}-\frac{{\bf
p}^2}{8m_b^2}
\Big(1+\frac{3(\varepsilon_a+m_a)}{2m_b}\Big)\Big)
\frac{\varepsilon_q}{M_A}({\bf p}\overleftarrow
{\frac{\partial}{\partial{\bf p}}})\Bigg]\Psi_B({\bf p}),\\
\label{44}
\nonumber
V^{(2)}_S(q^2_{max})&=&\frac{1}{M_A+M_B}\sqrt{\frac{M_A}{M_B}}\int\fra
{(2\pi)^3}\bar\Psi_A({\bf
p})\left(\frac{\varepsilon_a+m_a}{2\varepsilon_a}
\right)^{1/2}\frac{1}{2\varepsilon_a}\Bigg[-\frac{M_B-\varepsilon_b
-\varepsilon_q}{\varepsilon_a}\\
\nonumber
&&+\frac{{\bf p}^2}{6}\Big(\frac{1}{\varepsilon_a^2}-
\frac{1}{m_b^2}\Big)-
\frac{\varepsilon_a}{6}\big(M_B+M_A-\varepsilon_b-\varepsilon_a-
2\varepsilon_q\big)\\
&&\times\Big(\frac{1}{\varepsilon_a^2}-
\frac{1}{m_b^2}\Big)\frac{\varepsilon_q}
{M_A}({\bf p}\overleftarrow
{\frac{\partial}{\partial{\bf p}}})\Bigg]\Psi_B({\bf p}),\\
\label{45}
\nonumber
V^{(2)}_V(q^2_{max})&=&\frac{1}{M_A+M_B}\sqrt{\frac{M_A}{M_B}}\int\fra
{(2\pi)^3}\bar\Psi_A({\bf
p})\left(\frac{\varepsilon_a+m_a}{2\varepsilon_a}
\right)^{1/2}\frac{1}{2\varepsilon_a}\Bigg[\Big(\frac{{\bf p}^2}{6}
+\frac{\varepsilon_a}{6}\\
\nonumber
&&\times\big(M_B-M_A-\varepsilon_b+\varepsilon_a\big)
\times\frac{\varepsilon_q}{M_A}({\bf
p}\overleftarrow{\frac{\partial}{\partial
{\bf p}}})\Big)
(1+\kappa)\Big(\frac{1}{\varepsilon_a^2}+\frac{1}{m_b^2}-
\frac{1}{\varepsilon_q}\Big(\frac{2}{\varepsilon_a+m_a}+
\frac{1}{m_b}\Big)\Big)\\
\nonumber
&&-\frac{{\bf
p}^2\varepsilon_a}{6\varepsilon_q}\Big(\frac{2}{\varepsilon_a+m_a}
-\frac{1}{m_b}\Big)
+\frac{\varepsilon_a}{6M_A}
\big(M_B+M_A-\varepsilon_b-\varepsilon_a-2\varepsilon_q\big)\\
&&\times\Big(\frac{2}{\varepsilon_a+m_a}-\frac{1}{m_b}\Big)({\bf
p}\overleftarrow
{\frac{\partial}{\partial{\bf p}}})\Bigg]\Psi_B({\bf p}),
\end{eqnarray}
```

here $({\bf p}\overleftarrow{\partial/\partial{\bf p}})$ acts
to the left on the wave function $\bar\Psi_A({\bf p})$.
In the limit ${\bf p}^2/m^2\to 0$ the above form factors reduce to the
standard expressions, obtained in the nonrelativistic quark models.

Appendix B. Functions $K_{1,2,3}(x)$ for $(1/\Gamma)d\Gamma/dx$ Differential Distributions

a) In the case of $0^- \to 0^-$ transition

$$K_1(x) = \frac{2M_A}{M_B}x(1-2x)(1-R)|f_+(1)|^2, \tag{68}$$

$$K_2(x) = \frac{2M_A}{M_B}\left(1+\frac{M_A}{M_B}\right)^2(1-2x)|f_+(1)|^2, \tag{69}$$

$$K_3(x) = \frac{M_A}{M_B}\left(\rho+(1-2x)^2+\frac{2M_A}{M_B}(1-2x)-\frac{4M_A}{M_B}\alpha(1-2x)\right)|f_+(1)|^2. \tag{70}$$

b) In the case of $0^- \to 1^-$ transition

$$\begin{aligned}K_1(x) &= \frac{M_B}{M_A}x(1-R)\big(G_1(x)+\alpha G_2(x)+\frac{2}{3}\alpha^2G_3(x)\big)+\frac{1}{2}\big(G_2(x)+\frac{2}{3}\alpha G_3(x)\big)\\ &\times\Big(x(1-r)\big(1+\frac{M_B}{M_A}\big)^2-\frac{M_B^2}{M_A^2}x^2(1-R)^2\Big)+\frac{1}{3}G_3(x)\Big(\frac{3M_B}{M_A}x(1-R)\frac{(M_A+M_B)^4}{4M_A^2M_B^2}\\ &+\frac{3M_B^2}{M_A^2}\Big(\frac{M_A+M_B}{2M_AM_B}\Big)^2x^2(1-R)^2-\Big(\frac{M_A+M_B}{8M_A^3M_B^3}\Big)^6x^3(1-R)^3\Big),\end{aligned} \tag{71}$$

$$\begin{aligned}K_2(x) &= -\frac{(M_A+M_B)^2}{M_AM_B}\big(G_1(x)+\alpha G_2(x)+\frac{2}{3}\alpha^2G_3(x)\big)\\ &-\frac{(M_A+M_B)^4}{M_A^2M_B^2}\big(G_2(x)+\frac{2}{3}\alpha G_3(x)\big)-\frac{(M_A+M_B)^6}{12M_A^3M_B^3}G_3(x),\end{aligned} \tag{72}$$

$$K_3(x) = -G_4(x)-2\alpha G_1(x)-2\alpha^2G_2(x)-\frac{4}{3}\alpha^3G_3(x), \tag{73}$$

where $G_{1,2,3,4}(x)$ depend on the values of form factors at $w=1$ point

$$\begin{aligned}G_1(x) &= V^2(1)\Big(\frac{16M_A^2}{(M_A+M_B)^2}\Big(1-2x+\frac{M_A}{M_B}\Big)^2-\frac{16M_A^2}{M_B^2}\Big(1-2x+\frac{2M_A}{M_B}\Big)\Big)\\ &+\frac{16M_AM_B}{(M_A+M_B)^2}A_2^2(1)\Big(1-2x+\frac{M_A}{M_B}\Big)^2-\frac{8M_A}{M_B}A_1(1)V(1)\Big(1+\frac{M_A}{M_B}\Big)^2\Big(1-2x+\frac{M_A}{M_B}\Big)\\ &-\frac{4M_A}{M_B}A_1(1)A_2(1)\Big(1+\frac{M_B}{M_A}\Big)\Big(1-2x+\frac{M_A}{M_B}\Big)^2,\end{aligned} \tag{74}$$

$$\begin{aligned}G_2(x) &= \frac{16M_A^2}{(M_A+M_B)^2}\frac{M_A}{M_B}V^2(1)\Big(2(1-2x)+\big(1+\frac{M_A}{M_B}\big)^2+\frac{4M_A}{M_B}\Big)-\frac{8M_AM_B}{(M_A+M_B)^2}A_2^2(1)\\ &\times\Big(\big(1-2x+\frac{M_A}{M_B}\big)^2+\frac{4M_A}{M_B}(1-2x)\Big)+\frac{M_A}{M_B}A_1^2(1)\big(1+\frac{M_A}{M_B}\big)^2\Big(\big(1+\frac{M_A}{M_B}\big)^2\\ &\times\frac{M_B^2}{2M_A^2}\big(1-2x+\frac{M_A}{M_B}\big)^2\Big)+\frac{8M_A^2}{M_B^2}A_1(1)V(1)\Big(2(1-2x)+\big(1+\frac{M_A}{M_B}\big)^2+\frac{2M_A}{M_B}\Big)\end{aligned}$$

$$+4A_1(1)A_2(1)\Big(1-2x+\frac{M_A}{M_B}\Big)^2+\frac{8M_A}{M_B}A_2(1)A_1(1)(1-2x)\Big(1+\frac{M_A}{M_B}\Big), \tag{75}$$

$$G_3(x) = -\frac{8M_A}{M_B}A_1(1)A_2(1)(1-2x)-\frac{16M_A^3}{M_B^3}A_1(1)V(1)+\frac{16M_A^2}{(M_A+M_B)^2}\Big(A_2^2(1)(1-2x)$$
$$-\frac{2M_A^2}{M_B^2}V^2(1)\Big)+\frac{2M_A^2}{M_B^2}\Big(1+\frac{M_A}{M_B}\Big)^2A_1^2(1)\Big(-1+\frac{M_B^2}{2M_A^2}(1-2x)\Big), \tag{76}$$

$$G_4(x) = \frac{8M_AM_B}{(M_A+M_B)^2}V^2(1)\Big(1+\frac{M_A}{M_B}\Big)\Big(1-2x+\frac{M_A}{M_B}\Big)^2. \tag{77}$$

References

[1] N.Isgur, D.Scora, B.Grinstein and M.B.Wise, Phys.Rev.D39, 799 (1989).

[2] M.Wirbel, B.Stech and M.Bauer, Z.Phys.C29, 627 (1985); Z.Phys.C42, 671 (1989).

[3] T.Altomari and L.Wolfstein, Phys.Rev.D37, 681 (1988).

[4] C.Bernard, A.El.Khadra and A.Soni, Phys.Rev.D43, 2140 (1992).

[5] V.Lubicz, G.Martinelli, M.S.McArthy and C.T.Sachrajda, Phys.Lett.B274, 415 (1992).

[6] P.Ball, V.M.Braun and H.G.Dosch, Phys.Rev.D44, 3567 (1991).

[7] M.Neubert, Phys.Rep.245, 259 (1994).

[8] R.N.Faustov and V.O.Galkin, Z.Phys.C in press.

[9] V.O.Galkin, A.Yu.Mishurov and R.N.Faustov, Yad.Fiz. 55, 2175 (1992).

[10] V.O.Galkin, A.Yu.Mishurov and R.N.Faustov, Yad.Fiz. 51, 1101 (1990).

[11] V.O.Galkin, A.Yu.Mishurov and R.N.Faustov, Yad.Fiz. 53, 1676 (1991).

[12] R.N.Faustov and V.O.Galkin, preprint E2-94-438, Dubna, (1994); hep-ph/9505387.

[13] R.N.Faustov, V.O.Galkin and A.Yu.Mishurov, Proc. Seventh Int. Seminar 'Quarks-92', eds. D.Yu.Grigoriev et al., Singapore: World Scientific, 326 (1993).

[14] V.O.Galkin, A.Yu.Mishurov and R.N.Faustov, Yad.Fiz. 55, 1080 (1992).

[15] A.A.Logunov and A.N.Tavkhelidze, Nuovo.Cim. 29, 380 (1963).

[16] A.P.Martynenko and R.N.Faustov, Teor.Mat.Fiz. 64, 179 (1985).

[17] D.Gromes, Nucl.Phys.B131, 80 (1977).

[18] H.Schnitzer, Phys.Rev.D18, 3482 (1978).

[19] R.N.Faustov, Ann.Phys. 78, 176 (1973); Nuovo.Cim. 69, 37 (1970).

[20] V.O.Galkin and R.N.Faustov, Teor.Mat.Fiz. 85, 155 (1990).

[21] F.Gilman and R.J.Singelton, Phys.Rev.D41, 142 (1990).

[22] Particle Data Group, Phys.Rev.D50, 1173, (1994).

[23] CLEO: S.Sanghera et al., Phys.Rev.D47, 791 (1993).

[24] N.Isgur and M.B.Wise, Phys.Lett.B237, 527 (1990).

[25] M.Neubert et al., in Heavy Flavors, ed. by A.J.Buras and M.Lindner, Advanced Series on Directions in High Energy Physics, Singapore: World Scientific, (1994).

[26] ARGUS: H.Albrecht et al., Phys.Lett.B229, 175 (1989).

[27] CLEO: R.Fulton et al., Phys.Rev.D43, 651 (1991).

[28] ARGUS: H.Albrecht et al., Z.Phys.C57, 533 (1993).

[29] CLEO: D.Bortoletto et al., Phys.Rev.Lett.63, 1667 (1989).

[30] E691: J.C.Anjos et al., Phys.Rev.Lett.65, 2630 (1990).

[31] E653: K.Kodama et al., Phys.Lett.B286, 187 (1992).

[32] E687: P.L.Frabetti et al., Phys.Lett.B307, 262 (1993).

[33] CLEO: A.Bean et al., Phys.Lett.b317, 647 (1993).

[34] V.O.Galkin, A.Yu.Mishurov and R.N.Faustov, hep- ph/9505321, submitted to Phys.Lett.B

[35] CLEO: Phys.Lett.B337, 405 (1994).

[36] E653: Mod.Phys.Lett.A9, 675 (1994).

Table 1. Theoretical predictions and experimental data for form factors in $D \to Kl\nu_l$ and $D \to D^* l\nu_l$.

Ref.	$f_+(0)$	$V_0(0)$	$A_1(0)$	$A_2(0)$
Exp. Average [22]	$0.75 \pm 0.02 \pm 0.02$	1.1 ± 0.2	0.56 ± 0.04	0.40 ± 0.08
Theory				
RQM	0.73	0.62	0.63	0.43
ISGW [1]	0.82	1.1	0.8	0.8
BSW [2]	0.76	1.3	0.88	1.2
AW [3]	0.7	1.5	0.8	0.6
BKS [4]	$0.9 \pm 0.08 \pm 0.21$	$1.4 \pm 0.5 \pm 0.5$	$0.8 \pm 0.1 \pm 0.3$	$0.6 \pm 0.1 \pm 0.2$
LMMS [5]	0.63 ± 0.08	0.9 ± 0.1	0.53 ± 0.03	0.2 ± 0.2
BBD [6]	0.6	1.1	0.5	0.6

Table 2. Calculated and measured $D \to K^* l\nu_l$ form factor ratios $R_2 = A_2(0)/A_1(0)$ and $R_V = V(0)/A_1(0)$.

Ref.	$R_2(0)$	$R_V(0)$
Experiment		
E691 [30]	$0.0 \pm 0.5 \pm 0.2$	$2.0 \pm 0.6 \pm 0.3$
E653 [31]	$0.82^{+0.22}_{-0.23} \pm 0.11$	$2.00^{+0.34}_{-0.32} \pm 0.16$
E687 [32]	$0.78 \pm 0.18 \pm 0.10$	$1.74 \pm 0.27 \pm 0.28$
Theory		
RQM	0.68	0.98
ISGW [1]	1.0	1.37
BSW [2]	1.36	1.48
AW [3]	0.75	1.87
BBD [6]	1.2	2.2

Table 3. The ratios $\Gamma(D \to K^* l\nu_l)/\Gamma(D \to Kl\nu_l)$ and Γ_L/Γ_T in comparison with the experimental data.

Ref.	$\Gamma(K^*)/\Gamma(K)$	Γ_L/Γ_T
RQM	0.65	1.05
Experiment		
E691 [30]		$1.8^{+0.6}_{-0.4} \pm 0.3$
E653 [31]		$1.18 \pm 0.18 \pm 0.08$
E687 [32]		$1.20 \pm 0.13 \pm 0.13$
CLEO [33]	$0.60 \pm 0.09 \pm 0.07$	
CLEO [33]	$0.65 \pm 0.09 \pm 0.10$	

Table 4. Measured and calculated ratios of form factors in $D_s \to \phi l \nu_l$.

Ref.	$R_2(0)$	$R_V(0)$
Exp. Average [22]	1.8 ± 0.5	2.0 ± 0.7
CLEO [35]	$1.4 \pm 0.5 \pm 0.3$	$0.9 \pm 0.6 \pm 0.3$
E653 [36]	$2.1^{+0.6}_{-0.5} \pm 0.2$	$2.3^{+1.1}_{-0.9} \pm 0.4$
Theory		
RQM	0.55	0.94
BKS [4]	$2.0 \pm 0.19 \pm 0.23$	$0.78 \pm 0.08 \pm 0.15$
LMMS [5]	1.65 ± 0.2	0.33 ± 0.36

Table 5. Predicted and measured ratios of form factors in $B \to D^* l \nu_l$ at $q^2 = q^2_{max}$.

Ref.	$R_2(q^2_{max})$	$R_V(q^2_{max})$
Experiment		
CLEO [23] a)	1.02 ± 0.24	1.07 ± 0.57
CLEO [23] b)	0.79 ± 0.28	1.32 ± 0.62
Theory		
RQM	1.16	1.74
ISGW [1]	1.14	1.27
WSB [2]	1.06	1.14
HQET-based [24]	1.26	1.26
HQET-based [25]	1.14	1.74

Figure Captions

Fig.1 Lowest order vertex function.

Fig.2 Vertex function with account of the quark interaction. Dashed line corresponds to the effective potential (5). Bold line denotes the negative-energy part of quark propagator.

Fig.3 Allowed region for semileptonic $B \to A(A^*) l \nu_l$ decay in terms of the variables w and x. Lower bound curve $w_m(x)$ is determined by (64), upper bound is $w_0 = (M_A^2 + M_B^2)/(2M_A M_B)$.

Fig.4 $(1/\Gamma)(d\Gamma/dx)$ for $B \to D l \nu_l$ and $B \to D^* l \nu_l$. Absolute rates $d\Gamma/dx$ can be obtained by using $\Gamma(D) = 1.71 \times 10^{10} s^{-1}$ and $\Gamma(D^*) = 2.92 \times 10^{10} s^{-1}$ for $\tau_{B^0} = 1.5 \times 10^{-12}$ and $|V_{bc}| = 0.036$.

Fig.5 $(1/\Gamma)(d\Gamma/dx)$ for $D \to K l \nu_l$ and $D \to K^* l \nu_l$. Absolute rates $d\Gamma/dx$ can be obtained by using $\Gamma(K) = 6.68 \times 10^{10} s^{-1}$ and $\Gamma(K^*) = 4.34 \times 10^{10} s^{-1}$ for $\tau_{D^0} = 0.415 \times 10^{-12} s$, $\tau_{D^+} = 1.06 \times 10^{-12} s$.

Fig.6 $(1/\Gamma)(d\Gamma/dx)$ for $D_s \to \phi l \nu_l$. Absolute rate $d\Gamma/dx$ can be obtained by using $\Gamma = 5.42 \times 10^{10} s^{-1}$ for $\tau_{D_s} = 0.47 \times 10^{-12} s$.

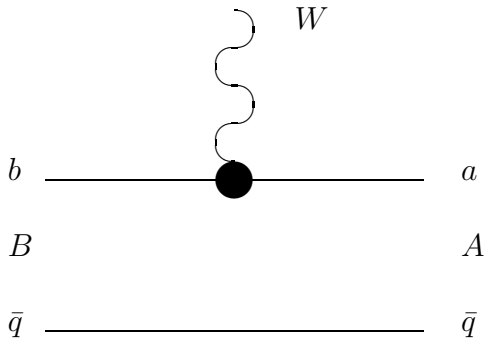

Fig. 1

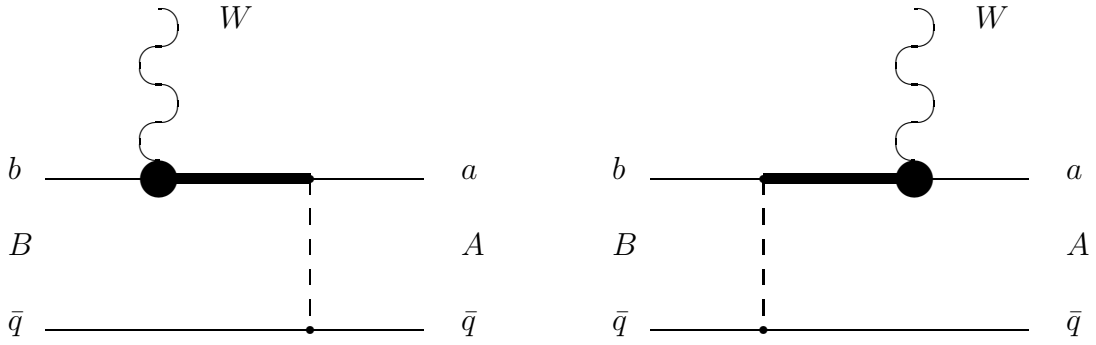

Fig. 2

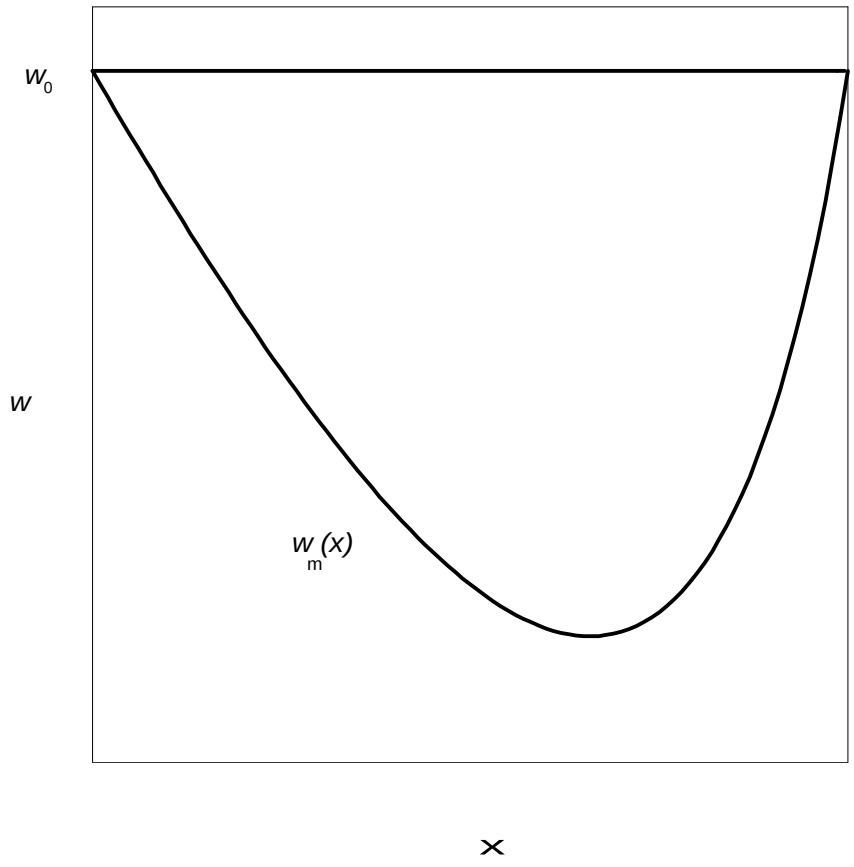

Fig. 3

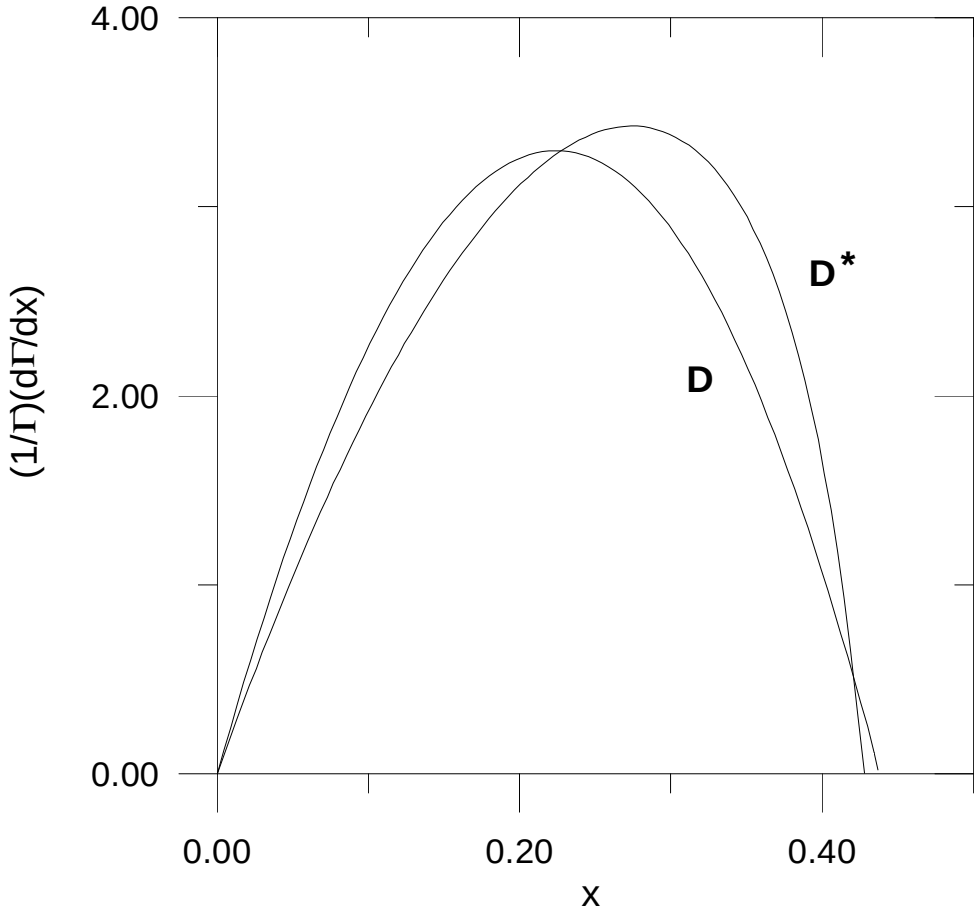

Fig.4

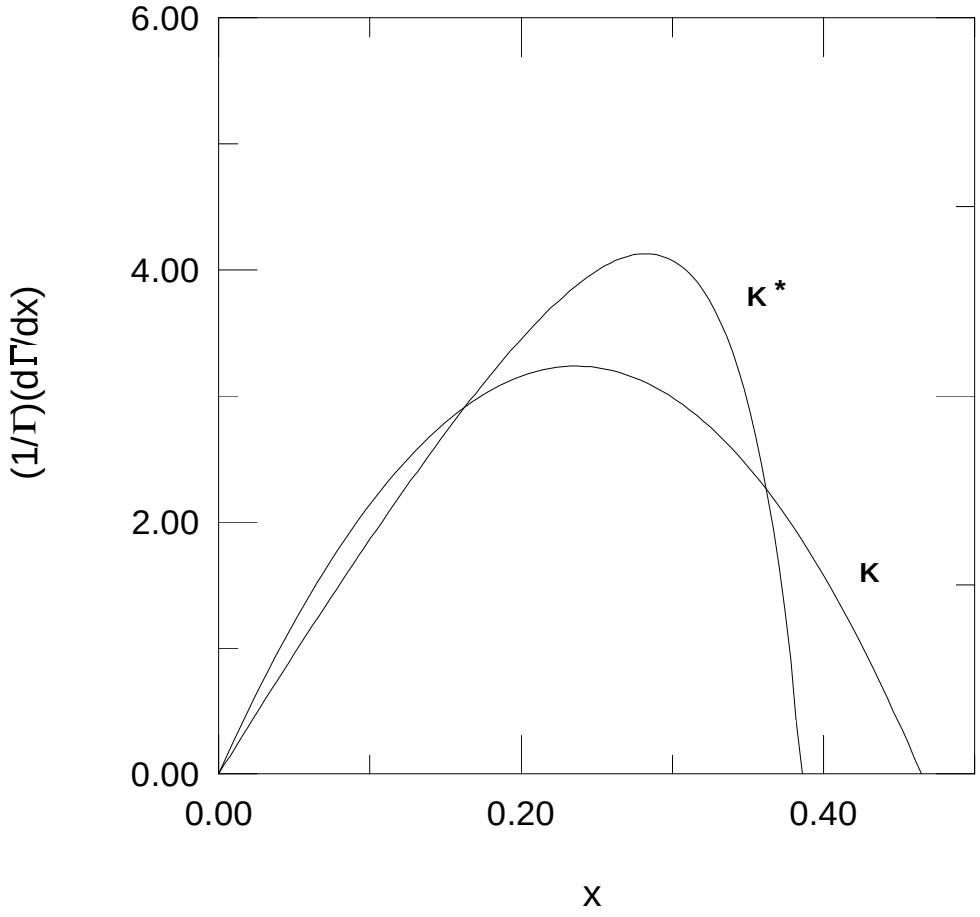

Fig.5

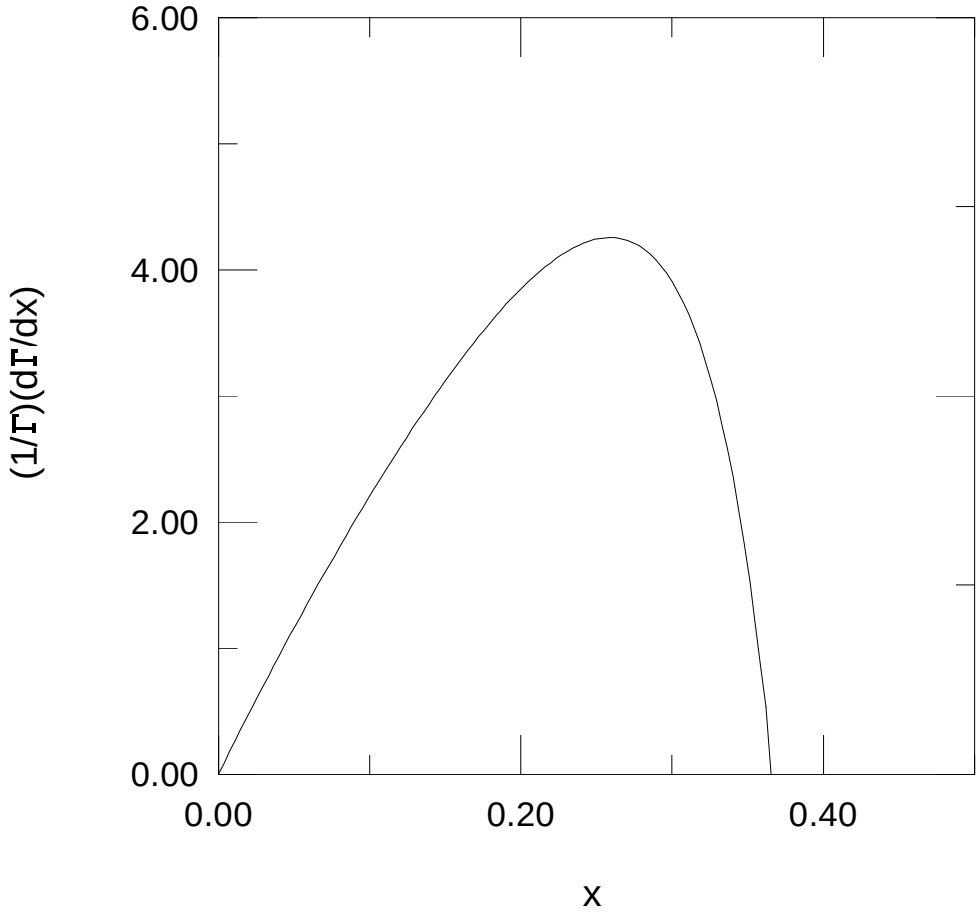

Fig.6